Journal of Solid State Chemistry 228 (2015) 208–213

Contents lists available at ScienceDirect

Journal of Solid State Chemistry

journal homepage: www.elsevier.com/locate/jssc

Synthesis and characterization of $La_{0.6}Sr_{0.4}Fe_{0.8}Cu_{0.2}O_{3-\delta}$ oxide as cathode for Intermediate Temperature Solid Oxide Fuel Cells

Santiago Vázquez [a], Sebastián Davyt [a], Juan F. Basbus [b], Analía L. Soldati [b], Alejandro Amaya [c], Adriana Serquis [b], Ricardo Faccio [a], Leopoldo Suescun [a,*]

[a] Laboratorio de Cristalografía, Estado Sólido y Materiales, DETEMA, Facultad de Química, UdelaR, Gral. Flores 2124, Montevideo, Uruguay
[b] Grupo Caracterización de Materiales, CAB-CNEA, Bustillo 9500, 8400 Bariloche, Argentina
[c] Laboratorio de Fisicoquímica de Superficies, DETEMA, Facultad de Química, UdelaR, Gral. Flores 2124, Montevideo, Uruguay

ARTICLE INFO

Article history:
Received 20 January 2015
Received in revised form
18 April 2015
Accepted 26 April 2015
Available online 6 May 2015

Keywords:
IT-SOFC
Cathode
Perovskite
Gel combustion

ABSTRACT

Nanocrystalline $La_{0.6}Sr_{0.4}Fe_{0.8}Cu_{0.2}O_{3-\delta}$ (LSFCu) material was synthetized by combustion method using EDTA as fuel/chelating agent and NH_4NO_3 as combustion promoter. Structural characterization using thermodiffraction data allowed to determine a reversible phase transition at 425 °C from a low temperature *R-3c* phase to a high temperature *Pm-3m* phase and to calculate the thermal expansion coefficient (TEC) of both phases. Important characteristics for cathode application as electronic conductivity and chemical compatibility with $Ce_{0.9}Gd_{0.1}O_{2-\delta}$ (CGO) electrolyte were evaluated. LSFCu presented a p-type conductor behavior with maximum conductivity of 135 S cm^{-1} at 275 °C and showed a good stability with CGO electrolyte at high temperatures. This work confirmed that as prepared LSFCu has excellent microstructural characteristics and an electrical conductivity between 100 and 60 S cm^{-1} in the 500–700 °C range which is sufficiently high to work as intermediate temperature Solid Oxide Fuel Cells (IT-SOFCs) cathode. However a change in the thermal expansion coefficient consistent with a small oxygen loss process may affect the electrode-electrolyte interface during fabrication and operation of a SOFC.

© 2015 Elsevier Inc. All rights reserved.

1. Introduction

Solid Oxide Fuel Cells (SOFCs) are electrochemical devices considered as one of the most promising candidates for power generation from large stationary plants to small and portable distributed generation applications with superior benefits than other fuel cells [1]. Nowadays there is a great interest on developing Intermediate Temperature Solid Oxide Fuel Cells (IT-SOFCs) working in the 500–700 °C temperature range [2]. One of the main research topics is the development of highly active and long term stable cathodes for IT-SOFCs. Moreover lowering the operating temperature reduces electrode kinetics and increases the interfacial polarization resistances, particularly on the cathode side of the cell. As a consequence, a major effort is being made to enhance the cathode performance using different synthesis routes and compositions to obtain porous materials, with small particle sizes and high purity [3–5].

The best cathode materials that have been described so far are based on the simple perovskite structure $ABO_{3-\delta}$, with cation disorder in the *A* and *B* sites and a significant proportion of disordered oxygen vacancies. In most cases where B cations are multivalent, these materials are mixed ionic-electronic conductors (MIECs) favouring the reduction of the cathode area specific resistance (ASR) [6]. Some of the reported cathode materials with highest electrochemical activities for the oxygen reduction reaction (ORR) are compounds such as $(Ba,Sr)(Co,Fe)O_{3-\delta}$ (BSCF) [7–9], $(La,Sr)(Co,Fe)O_{3-\delta}$ (LSFC) [10] and $LnBaCo_2O_{5+\delta}$ [11]. The presence of the Co^{+3}/Co^{+4} pair in these perovskites enhance the ORR kinetics leading to a very low polarization loss. Nevertheless these cathode compositions with high cobalt content show large thermal expansion coefficients (TEC), larger than the ceria-based electrolytes (CGO: $Ce_{0.9}Gd_{0.1}O_{2-\delta}$ and CSO: $Ce_{0.9}Sm_{0.1}O_{2-\delta}$) and interconnector materials (ferritic stainless steel) available for IT-SOFCs applications limiting the cell life.

Recently, the preparation of cobalt-free cathodes [12,13] has taken much relevance and iron-based perovskite as $Ba_{0.5}Sr_{0.5}FeO_{3-\delta}$ and $La_{1-x}Sr_xFeO_{3-\delta}$ have attracted much attention due to its lower TEC and superior structural stability than cobalt-based materials [14,15]. Unfortunately, these materials present a lower activity due to the low

* Correspondence to: Cryssmat-Lab/Cátedra de Física/DETEMA, Facultad de Química, Av. Gral. Flores 2124, Casilla 1157, Montevideo 11800, Uruguay.
E-mail address: leopoldo@fq.edu.uy (L. Suescun).

http://dx.doi.org/10.1016/j.jssc.2015.04.044
0022-4596/© 2015 Elsevier Inc. All rights reserved.

electrical conductivity and oxygen permeation compared to cobalt-based perovskite [16]. Novel cathodes using copper as substituent have proven to be an interesting alternative since the presence of Cu^{+2}/Cu^{+3} in the structure instead of Fe^{+3}/Fe^{+4} increases the electronic conductivity, reduces the polarization resistance and increases the oxygen vacancies, which enables their use in IT-SOFC applications [17–20]. Additionally Cu-substituted Fe perovskites can be prepared at lower temperatures than pure Fe ones, allowing for a better control of the microstructure. $La_{0.6}Sr_{0.4}Fe_{0.8}Cu_{0.2}O_{3-\delta}$ was reported as a novel cathode material by Zhou et al. [19] as substituent and demonstrate to be a promising material for IT-SOFC with high electrical conductivity, low polarization resistance for oxygen reduction reaction (ORR) and thermal expansion coefficient (TEC) similar to ceria-based electrolytes.

Here we describe a modified gel combustion route using EDTA as fuel/complexation agent and assisted with NH_4NO_3 which has proven to be a good method for preparing nanocrystalline oxides [20]. This synthesis method was used successfully to prepare nanocrystalline $La_{0.6}Sr_{0.4}Fe_{0.8}Cu_{0.2}O_{3-\delta}$ (LSFCu) powders. A detailed microstructural characterization was performed by Transmission Electron Microscopy (TEM) and the structure and thermal expansion coefficients were studied using synchrotron X-ray diffraction data at different temperatures. Additionally, important parameters for SOFC-cathode application, such as electrical conductivity and chemical compatibility with $Ce_{0.9}Gd_{0.1}O_{2-\delta}$ electrolyte are presented.

2. Materials and methods

2.1. Synthesis of $La_{0.6}Sr_{0.4}Fe_{0.8}Cu_{0.2}O_{3-\delta}$ powder

$La_{0.6}Sr_{0.4}Fe_{0.8}Cu_{0.2}O_{3-\delta}$ (LSFCu) powder was prepared by a modified gel combustion route, using ethylenediaminetetraacetic acid (EDTA) as fuel and complexation agent. In gel combustion routes the most used fuels are glycine, citric acid and urea, due to their ability to form stable complexes with metal ions and because they prevent the precipitation of metal ions during the water evaporation process [21]. Additionally these compounds self-ignite at high temperature providing the needed start of the combustion process.

We use EDTA in basic medium (pH = 10) that is a stronger titration agent than glycine and urea, but does not ignite upon heating below 350 °C, so it is necessary to employ NH_4NO_3 as combustion promoter to enhance the auto-ignition and self-sustained combustion.

The synthesis of 5 g of LSFCu was performed using $La(NO_3)_3 \cdot 6H_2O$, $Sr(NO_3)_2$, $Fe(C_5H_7O_2)_2$ and $Cu(NO_3)_2 \cdot 3H_2O$ (all > 99.9%, from Sigma-Aldrich) as metal sources. The reagents were dissolved in stoichiometric amounts in 100 ml distilled water in a 800 ml beaker and EDTA was added as complexation agent. The EDTA/metal ion ratio was 1:1.1 (10% of EDTA in excess) to ensure the complete complexation of the cations HNO_3 (70%) and NH_4OH (28–30%) were added to form NH_4NO_3 in-situ and promote the combustion of EDTA. The solution with pH = 10 was heated over a hot plate with constant stirring at 150 °C until the gel was formed. The stirring bar was then removed from the dark-red gel that was posteriorly heated at 350 °C until self-ignition. The optimized quantities of HNO_3 and NH_4OH for this synthesis were 1.2 ml HNO_3/g EDTA and 3.5 ml NH_4OH/g EDTA. This proportion was found high enough to promote the full combustion of the gel but low enough to prevent an explosive combustion, due to the highly exothermic decomposition of NH_4NO_3. As final step the obtained ashes were pressed in 13 mm pellets at 25 MPa and fired at 900 °C for 5 h with a heating rate of 5 °C min^{-1} to obtain fine nanocrystalline LSFCu powders.

2.2. Transmission electron microscopy characterization

Morphological characterization and electron diffraction of cathode powder was performed by transmission electron microscopy (TEM) using a Philips CM 200 UT instrument with a LaB_6 filament operated at 200 kV. Some mg of the powdered samples were suspended in isopropyl alcohol and ultrasonicated for 5 min, a drop of the liquid was transferred into a Ultrathin/Holey Carbon film coated gold TEM grid of 300 Mesh (Ted Pella INC.) and allowed to dry in air.

2.3. Synchrotron X-ray thermodiffraction

The LSFCu sample was characterized by thermodiffraction from RT to 900 °C in air atmosphere using the ARARA furnace at D10B-XPD beamline of the Brazilian Synchrotron Light Laboratory (LNLS). The beamline is equipped with a θ–2θ reflection-geometry diffractometer with a Mythen 1000 linear position sensitive detector (PSD).

X-rays with energies of 10 keV and 7.13 keV ($\lambda_{10\ keV} = 1.24058$ Å and $\lambda_{7.13\ keV} = 1.74016$ Å) were used to illuminate the sample mounted in a spinning flat holder during data collection in the $2\theta = 10$–$120°$ range in steps of 0.5°. The detector, spanning 3°, collected data six times at each 2θ value. Data reduction and averaging was carried out to obtain a powder pattern with a 2θ step = 0.005°. Rietveld refinement was used to characterize the structure of the observed phases and extract structural parameters for thermal expansion coefficient (TEC) determination. The pattern was fitted using the FullProf Suite including anomalous scattering (f' and f'') corrections for all atomic species for 10 keV and 7.13 keV incident radiation [22].

2.4. Thermogravimetric analysis

Thermogravimetric analysis (TGA) was performed to determine the oxygen loss of the LSFCu sample between RT and 850 °C in air atmosphere on a Shimadzu TGA-50 analyser. The sample was mounted in a platinum crucible and heated at 5 °C/min in a synthetic air flow of 50 ml/min.

2.5. Electrical conductivity

The electrical conductivity of LSFCu was studied using the standard DC four-probe technique with an Agilent Digital multimeter (model 34401A) from RT to 850 °C. LSFCu was prepared pressing the powder in disks of 13 mm at 25 MPa and then annealed at 1000 °C for 12 h to obtain dense pellets. The data collection was performed on quasi static conditions with a heating rate of 1 °C/min without airflow.

2.6. Chemical compatibility

X-ray diffraction (XRD) patterns were recorded to study the cathode-electrolyte chemical compatibility using a conventional powder diffractometer (Rigaku Ultima IV, operating at 40 kV and 30 mA using Cu$K\alpha$ radiation) operating in θ–θ Bragg–Brentano geometry. Powdered mixtures of LSFCu with CGO in the ratio 70/30 (wt%) were ground in agate mortar, pressed in to pellets and fired at 900 °C for 24, 48 and 120 h. The scans were performed in the 2θ range of 20–70° with a 0.04° step and a time collection step of 2 s.

3. Results and discussion

The material $La_{0.6}Sr_{0.4}Fe_{0.8}Cu_{0.2}O_{3-\delta}$ has a perovskite-type structure with La and Sr sharing the *A*-site and Fe and Cu the

B-site. This compound presents the rhombohedral *R-3c* (#167) space group at room temperature as described by Zhou et al., corresponding to a tilt of the oxygen octahedral described as $a^-a^-a^-$ following the Glazer's notation [23].

3.1. Synthesis and TEM characterization

We performed TEM characterization in order to study the morphology and particle size distribution of the synthesized LSFCu powders and to verify the symmetry of the perovskite structure at the local scale. Fig. 1a and b shows images of LSFCu nanoparticles and Fig. 1c a particle size histogram with a Gaussian size distribution with an average of 41 ± 25 nm obtained from gel combustion synthesis route. Generally, the combustion gel route gives broader particle size distributions due to the uncontrolled and exothermic process, so it is remarkable that our gel combustion route with EDTA and assisted with NH_4NO_3 allows to obtain homogeneous materials in high purity by a rapid synthetic route.

3.2. Structural characterization and thermal analysis

In order to discard the presence of Fe and Cu ordering in the perovskite B-site we performed an anomalous X-ray diffraction experiment (AXRD) collecting diffraction data using X-ray energies at and away from the Fe K absorption edge (7.13 and 10.0 keV respectively). The simultaneous refinement of the two data sets using the Rietveld method and the appropriate atomic scattering factors corrections (f' and f'') showed that there is no improvement in the structural model by assuming any kind of Fe/Cu ordering, therefore Fe and Cu are confirmed to be disordered in the structure. Fig. 2a shows the 10.0 keV synchrotron X-ray powder diffraction pattern of LSFCu compound fitted by the Rietveld method at room temperature (RT) using the final disordered model in the *B*-site positions. Table 1 presents the results of the Rietveld refinement at RT for this refinement including goodness of fit parameters.

We performed the structural characterization in the temperature range between RT and 900 °C in order to determine the phase evolution in the relevant range for preparation and operation of an IT-SOFC and determine the thermal expansion coefficient (TEC) of the phase. LSFCu shows a reversible phase transition at 425 °C to the cubic *Pm-3m* space group typical of the simple perovskite structure. This phase transition has been described many times for simple or cation-disordered perovskites and is induced by the gradual reduction of the octahedral tilt from $a^-a^-a^-$ to $a^0a^0a^0$ cubic form. This phase transition not reported for the $La_{0.6}Sr_{0.4}Fe_{0.8}Cu_{0.2}O_{3-\delta}$ system by Zhou et al. [19] is 2nd order since a continuous phase transformation is observed with the rhombohedral splitting and superstructure peaks slowly disappearing with temperature as can be seen in Fig. 3a. Only two small isolated super-structure peaks at $2\theta = 30.6^\circ$ and 31.6°, in the RT pattern, differentiate the rhombohedral from the cubic phase, however the relative intensities of the main peaks and small peak splitting can be easily detected by the Rietveld method.

The thermal expansion coefficient (TEC) was calculated by evaluating the change in lattice parameters with temperature and is shown in Fig. 3b. TEC for rhombohedral structure was

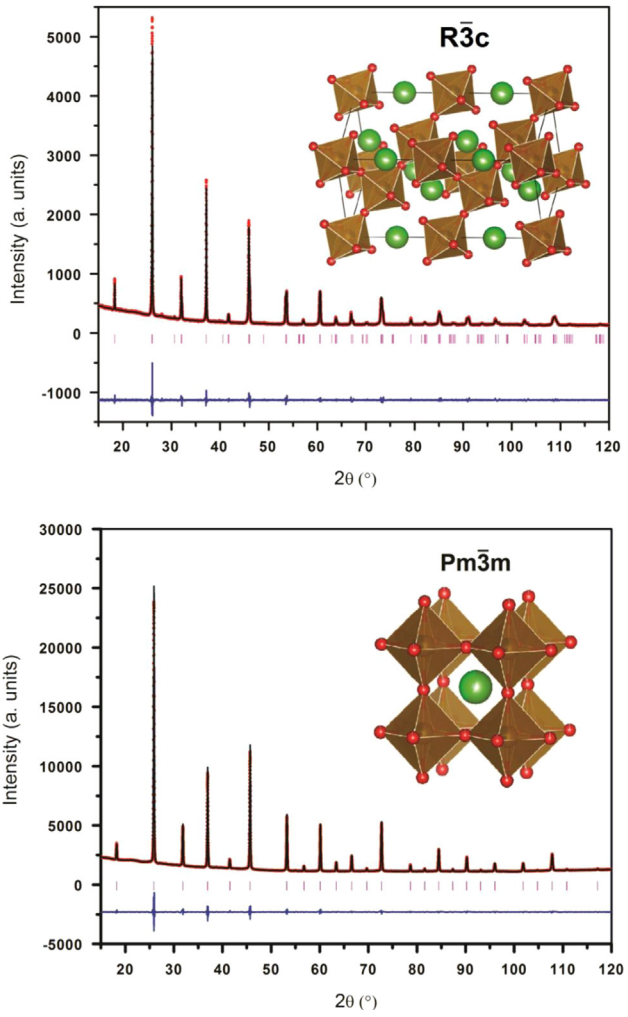

Fig. 2. Rietveld fit of XRD data of as-prepared LSFCu powder. Red dots are the observed intensities, the black line is the calculated intensity, vertical bars are peak positions for LSFCu: (a) rhombohedral phase at RT and (b) cubic phase at 450 °C. (For interpretation of the references to color in this figure legend, the reader is referred to the web version of this article.)

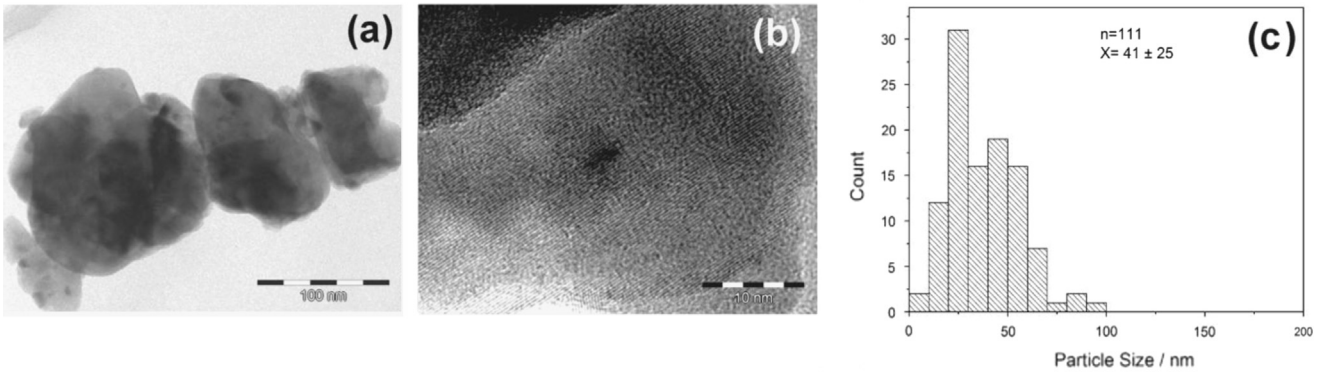

Fig. 1. (a) Dark field TEM image of nanoparticles, (b) high resolution TEM image where the crystal planes are shown and (c) particle size histogram.

Table 1
Refinement parameters.

Space group $R\bar{3}c$ (#167) T=25 °C		$a=b=5.51020$ (2) Å $c=13.42544$ (7) Å $\alpha=\beta=90°$ $\gamma=120°$			$\chi^2=1.87$ $Rp=19.1\%$ $Rwp=12.1\%$	
Atoms	***Wyckoff position***	***x***	***y***	***z***	***Occ.***	U_{iso} (Å^2)
La	**6*a***	**0**	**0**	**0.25**	**0.6**	**0.017 (2)**
Sr	**6*a***	**0**	**0**	**0.25**	**0.4**	**0.017 (2)**
Fe	**6*b***	**0**	**0**	**0**	**0.8**	**0.090 (3)**
Cu	**6*b***	**0**	**0**	**0**	**0.2**	**0.090 (3)**
O	**18*e***	**0.533 (1)**	**0**	**0.25**	**0.956 (2)**	**0.210 (6)**
Space group $Pm\bar{3}m$ (#221) T=450 °C		$a=b=c=3.91428$ (2) Å $\alpha=\beta=\gamma=90°$			$\chi^2=1.72$ $Rp=10.2\%$ $Rwp=6.56\%$	
Atoms	***Wyckoff position***	***x***	***y***	***z***	***Occ.***	U_{iso} (Å^2)
La	**1*b***	**0.5**	**0.5**	**0.5**	**0.6**	**0.01823 (6)**
Sr	**1*b***	**0.5**	**0.5**	**0.5**	**0.4**	**0.01823 (6)**
Fe	**1*a***	**0**	**0**	**0**	**0.8**	**0.0148 (1)**
Cu	**1*a***	**0**	**0**	**0**	**0.2**	**0.0148 (1)**
O	**3*d***	**0**	**0**	**0.5**	**0.978 (7)**	**0.031 (2)**

calculated plotting an average cell parameter (a_{ave}) between RT and 425 °C calculated with the normalized cell parameters of the rhombohedral cell respect to the ideal perovskite $a_P = a/\sqrt{2}$ and $c_P = c/2\sqrt{3}$ as $a_{ave} = (2a_P + c_P)/3$. For the range above 425 °C the cubic cell parameter (a_{cubic}) was plotted. The thermal expansion curve is composed of two linear portions and has a break near 425 °C that coincides with the phase transition. In the low temperature range the TEC attributed to the *R*-3*c* phase is 14.66×10^{-6} K^{-1} and in the higher temperature range the TEC attributed to the *Pm*-3*m* phase is 18.62×10^{-6} K^{-1}. The average TEC in the RT–900 °C range is 16.64×10^{-6} K^{-1} which slightly larger than the reported average TEC value using dilatometry 14.6×10^{-6} K^{-1} in the RT–800 °C [19].

Thermogravimetric analysis on LSFCu sample was performed in synthetic air to evaluate the oxygen loss and TGA results are shown in Fig. 4. The results between RT–250 °C show a fast weight loss that can be attributed to desorption of adsorbed water and other gasses [19]. In the 250–300 °C the weight is almost constant. The weight loss above 300 °C is primary due to the oxygen loss from the LSFCu structure and the formation of oxygen vacancies. This increment of the oxygen vacancies in the structure above 300 °C may be the cause of the phase transition that we reported at 425 °C. Also the oxygen loss from RT to 425 °C is about 0.25% and from 425 °C to 850 °C is about 1.5% that we consider may explain part of the change of slope in the TEC of the compound (so-called chemical expansion) above 425 °C, as can be observed for similar La–Sr ferrites doped with Cu and Co [24].

It is important to highlight than the TEC of CGO electrolyte is 12.5×10^{-6} K^{-1} [25] between 30 and 730 °C so the difference with LSFCu expansion is important. However the TEC of LSFCu is lower than Co-based perovskites as $Ba_{0.5}Sr_{0.5}Co_{0.8}Fe_{0.2}O_{3-\delta}$ [9]. The phase transition at 425 °C and significant change in TEC with temperature may be a disadvantage for this material that should sustain repetitive heating and cooling cycles during cell production, which may eventually lead to failure of mechanical contact with the electrolyte.

3.3. Conductivity

One of the most important requirements for cathode materials is a high electronic conductivity, preferable more than 100 S cm^{-1} under oxidizing atmosphere [26]. For this reason we measured the conductivity of LSFCu in the temperature range between RT and 850 °C with a heating rate of 1 °C/min. The conductivity of this sample increases with temperature, reaches a maximum value of 135 S cm^{-1} at 275 °C and then decays as shown in Fig. 5. The electrical conductivity is between 100 and 60 S cm^{-1} in the 500–700 °C range which is sufficiently high to work as cathode.

Similarly to other perovskites the LSFCu exhibits a semiconductor to metallic transition when the temperature is increased, due to a decrease of the p-type carriers produced by the oxygen loss. Previous reports for electrical conductivity characterization for LSFCu and similar compositions show discrepancies in the temperature of the transition. The semiconductor-metallic transition for $La_{0.6}Sr_{0.4}Fe_{0.8}Cu_{0.2}O_{3-\delta}$ was reported by Zhou at 575 °C [19], however for $La_{0.6}Sr_{0.4}Co_{0.1}Fe_{0.8}Cu_{0.1}O_{3-\delta}$ and $La_{0.6}Sr_{0.4}Co_{0.2}Fe_{0.7}Cu_{0.1}O_{3-\delta}$ the transition temperatures reported by Wang [24] were 350 °C and 400 °C respectively. The conductivity peak at low temperatures can be attributed to oxygen exchange that begins to create an increasing number of vacancies to compete with hole carriers. This could be expected due to the presence of Sr in the structure inducing the oxygen vacancy formation with tetravalent iron and trivalent copper according to [24,27]:

$$2[V_O^{\bullet\bullet}] + [Fe_{Fe}^{\bullet}] + [Cu_{Cu}^{\bullet}] = [Sr_{La}]$$

At temperatures lower than 275 °C the conductivity shows a thermally activated mechanism and increases with the temperature due to the increasing mobility of the electronic charge carriers, $Fe_{Fe}^{\bullet}$ and $Cu_{Cu}^{\bullet}$ which represents the holes localized in *B*-sites [24]. In this temperature range the conductivity can be represented by the thermally activated polaron-hopping mechanism expressed as $\sigma = (A/T)\exp(-E_a/k_BT)$. The calculated activation energy (E_a) for this mechanism was 0.068 eV.

3.4. Chemical compatibility with CGO

The chemical compatibility of cathode-electrolyte needs to be evaluated for technological development of SOFC materials. A previous report of chemical compatibility of LSFCu/SDC showed no decomposition reactions following the process by XRD [19]. Fig. 6 shows the XRD data for LSFCu/CGO mixtures fired at 950 °C for 24, 48 and 120 h. There is no evident reaction for these materials at 950 °C which is close to the symmetric cell preparation temperature and the highest of the process. This assures that the LSFCu/CGO interphase will not react at lower temperatures during cell operation

4. Conclusions

In this work we described a modified gel combustion route using EDTA and NH_4NO_3 that can be used to prepare easily and quickly

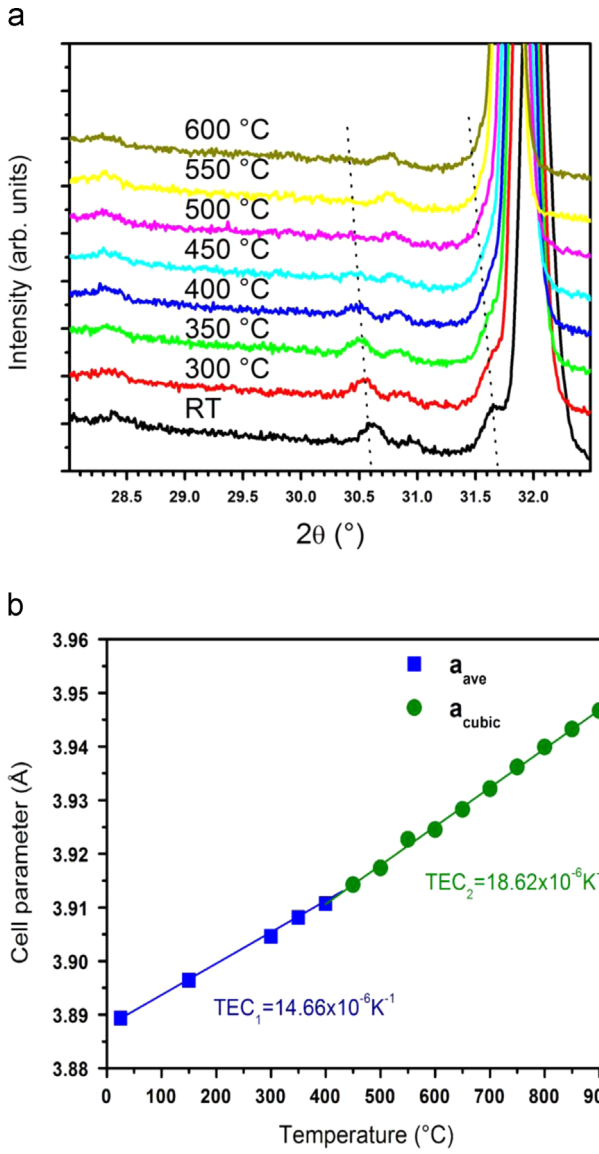

Fig. 3. (a) X-ray diffraction patterns for LSFCu at different temperatures and with $\lambda_{10\ keV}=1.24058$ Å. The data between RT and 400° corresponds to the $R\bar{3}c$ space group and the range between 450 and 600 °C corresponds to the $Pm\bar{3}m$ space group. (b) Thermal expansion coefficient determined from structural parameters. Note that two small peaks at ~27° and ~31° that show no change in intensity with temperature are due to a contribution from the beamline that is independent of the sample.

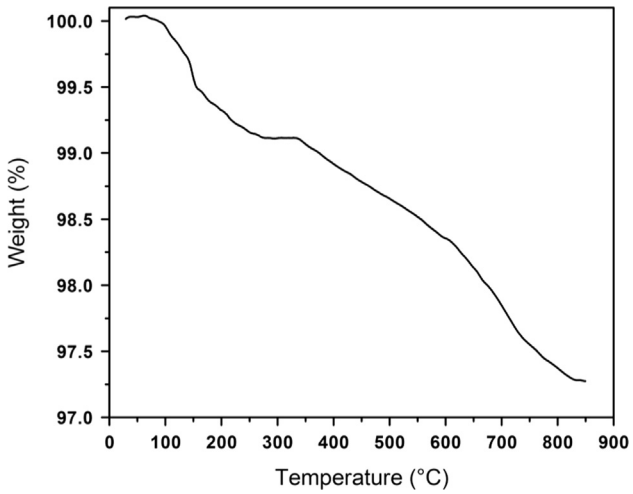

Fig. 4. Thermogravimetric analysis on the LSFCu material.

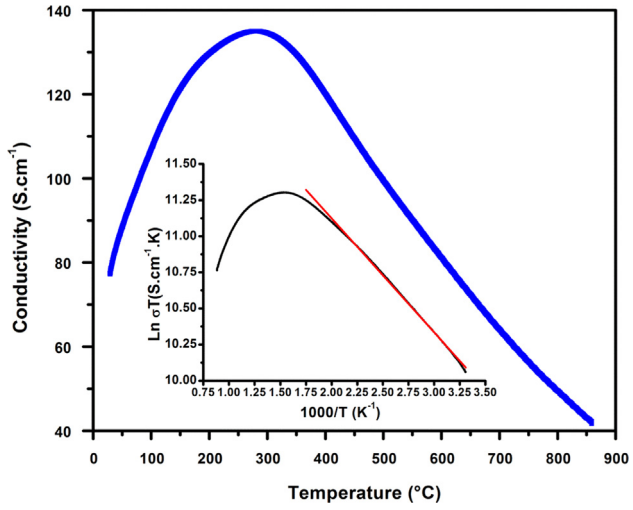

Fig. 5. Electronic conductivity vs. temperature graph, with a maximum conductivity of 135 S cm^{-1} at 275 °C. The inset shows the Arrhenius plot for conductivity.

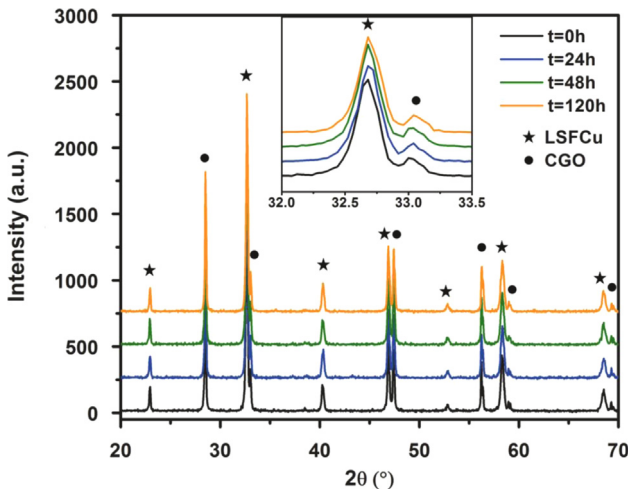

Fig. 6. Chemical stability of LSFCu/CGO mixtures at 950 °C.

nanocrystalline oxide materials. The $La_{0.6}Sr_{0.4}Fe_{0.8}Cu_{0.2}O_{3-\delta}$ (LSFCu) cathode material was synthesized using this method with an average particle size of 41 ± 25 nm.

A detailed structural characterization was performed showing a reversible phase transition $R\text{-}3c \leftrightarrow Pm\text{-}3m$ at 425 °C. The structural parameter between RT and 900 °C were used to determine a thermal expansion coefficient of $14.66 \times 10^{-6}\,K^{-1}$ in the RT–425 °C and $18.62 \times 10^{-6}\,K^{-1}$ in the 425–900 °C temperature ranges, and the average TEC is $16.64 \times 10^{-6}\,K^{-1}$. The LSFCu showed a lower average TEC than typical values for cobalt-based cathodes but the difference with the expansion of CGO electrolyte ($12.5 \times 10^{-6}\,K^{-1}$ in the 30–730 °C) is almost significant. Important characteristics for cathode application as electronic conductivity and chemical compatibility with CGO electrolyte were evaluated. LSFCu presented a p-type conductor behavior with maximum conductivity of 135 S cm^{-1} at 275 °C. LSFCu/CGO mixture exhibits chemical stability at 950 °C for 120 h demonstrating good stability for operation in IT-SOFCs devices. The results presented in this work and the high ORR activity reported by Zhou et al. [19] showed that LSFCu has good properties to work as IT-SOFC cathode despite its change in the TEC about 425 °C. A solution to

reduce the thermal expansion coefficient could be use this material in a composite cathode LSFCu/CGO that proved to be stable in the 500–700 °C temperature range.

Acknowledgments

This research was supported by Agencia Nacional de Investigación e Innovación (Uruguay) through grant FSE_2009_1_51, and Laboratorio Nacional de Luz Synchrotron (LNLS, Campinas, SP, Brazil) through a grant to perform research proposal XRD1-16057 at D10B-XPD beamline and PEDECIBA. Santiago Vázquez thanks for financial support of ANII POS_NAC_2014_1_102615 Ph. D. grant. This research effort was also funded by University of Cuyo, CNEA and ANPCyT-PICT (Argentina). The authors acknowledge to Dr. Alberto Caneiro for the use of his laboratories, to Dr. Horacio Troiani for his advice with the use of TEM and to Dr. K. Swierczek for helpful discussion.

References

[1] Arnab Choudhury, H. Chandra, A. Arora, Renew. Sustain. Energy Rev. 20 (2013) 430–442.
[2] Brian C.H. Steele, Angelika Heinzel, Nature 414 (2001) 345–352.
[3] Zongping Shao, Sossina M. Haile, Nature 431 (2004) 170–173.
[4] Rares Scurtu, Simona Somacescu, J. Solid State Chem. 210 (2014) 53–59.
[5] Analía L. Soldati, Laura Baqué, J. Solid State Chem. 198 (2013) 253–261.
[6] Stuart B. Adler, Chem. Rev. 104 (2004) 4791–4843.
[7] Wei Zhou, Ran Ran, Zongping Shao, J. Power Sources 192 (2009) 231–246.
[8] Bangwu Liu, Yue Zhang, Limin Zhang, Int. J. Hydrog. Energy 34 (1008–1014) (2009).
[9] H. Patra, S.K. Rout, S.K. Pratihar, S. Bhattacharya, Int. J. Hydrog. Energy 36 (2011) 11904–11913.
[10] Bo-Kuai Lai, Kian Kerman, Shriram Ramanathan, J. Power Sources 196 (2011) 1826–1832.
[11] S.L. Pang, et al., J. Power Sources 240 (2013) 54–59.
[12] Yingjie Niu, et al., J. Mater. Chem. 20 (2010) 9619–9622.
[13] Haihui Wang, Cristina Tablet, Armin Caro, Jurgen Feldhoff, Adv. Mater. 17 (2005) 1785–1788.
[14] Zhihao Chen, Ran Ran, Wei Zhou, Zongping Shao, Shaomin Liu, Electrochim. Acta 52 (2007) 7343–7351.
[15] S.P. Simner, et al., J. Power Sources 113 (2003) 1–10.
[16] Jae-Il Jung, Scott T. Misture, Doreen D. Edwards, J. Electroceram. 24 (2010) 261–269.
[17] Ling Zhao, et al., J. Power Sources 195 (2010) 1859–1861.
[18] Yihan Ling, et al., Int. J. Hydrog. Energy 35 (2010) 6905–6910.
[19] Qingjun Zhou, et al., Int. J. Hydrog. Energy 37 (2012) 11963–11968.
[20] Santiago Vázquez, et al., J. Power Sources 274 (2015) 318–323.
[21] Zongping Shao, Wei Zhou, Zhonghua Zhu, Prog. Mater. Sci. 57 (2012) 804–874.
[22] E. Prince, International Tables for Crystallography – Volume C, third edition, 2004.
[23] A.M. Glazer, Acta Crystallogr. B 28 (1972) 3384–3392.
[24] Sea-Fue Wang, et al., J. Power Sources 201 (2012) 18–25.
[25] Hideko Hayashi, et al., Solid State Ion. 132 (2000) 227–233.
[26] Chunwen Sun, Rob Hui, Justin Roller, J. Solid State Electrochem. 14 (2010) 1125–1144.
[27] W. Sitte, et al., Solid State Ion. 154–155 (2002) 517–522.